

## Letters to *Analytical Chemistry*

# Molecular Depth Profiling with Cluster Secondary Ion Mass Spectrometry and Wedges

Dan Mao,<sup>†</sup> Andreas Wucher,<sup>‡</sup> and Nicholas Winograd<sup>\*,†</sup>

Chemistry Department, Pennsylvania State University, 104 Chemistry Building, University Park, Pennsylvania 16802, and Faculty of Physics, University Duisburg-Essen, 47048 Duisburg, Germany

Secondary ion mass spectrometry and atomic force microscopy are employed to characterize a wedge-shaped crater eroded by 40 keV C<sub>60</sub><sup>+</sup> bombardment of a 395 nm thin film of Irganox 1010 doped with four delta layers of Irganox 3114. The wedge structure creates a laterally magnified cross section of the film. From an examination of the resulting surface, information about depth resolution, topography, and erosion rate can be obtained as a function of crater depth in a single experiment. This protocol provides a straightforward way to determine the parameters necessary to characterize molecular depth profiles and to obtain an accurate depth scale for erosion experiments.

Since it was first reported that cluster ion beams minimize the accumulation of beam-induced damage in a wide variety of organic materials,<sup>1</sup> secondary ion mass spectrometry (SIMS) experiments have been focused upon the implementation of molecular depth profiling and three-dimensional imaging as unique characterization tools in materials science. Depth information with a resolution to 10 nm has been achieved by correlating the amount of material removed, using tools such as the atomic force microscope (AFM), with the magnitude of the incident ion current and the time of bombardment.<sup>2</sup> Considerable information has been published recently regarding the ultimate achievable depth resolution.<sup>3,4</sup> Factors such as topography, ion beam mixing, temperature, incident beam angle and variations in the erosion rate have all been implicated in influencing the outcome of these experiments.<sup>5</sup> Although the parameters for molecular depth profiling are often very different than those associated with inorganic depth profiling

of atomic species,<sup>6</sup> some of the formalism developed more than 20 years ago is still applicable to these new systems.

An interesting strategy involves the sculpting of a wedge shaped crater using a focused ion beam (FIB) source. Beveling with very small slope angles has been employed to achieve laterally magnified cross sections of ion milled multilayer structures for many years using atomic solids.<sup>7</sup> More recently, Gillen and co-workers<sup>8</sup> utilized cluster bombardment and beveling to elucidate the structure of buried polymer interfaces, demonstrating, for the first time, the feasibility of using this idea for organic materials. It was suggested that a depth feature of 1 nm could easily be resolved with a 5  $\mu$ m SIMS probe.

The creation of wedge-shaped craters for the study of three-dimensionally complex materials is certainly intriguing from an imaging perspective, but here we suggest that by combining wedge technology with AFM measurements, fundamental information about the molecular depth profile may be acquired. To illustrate, we employ a C<sub>60</sub><sup>+</sup> projectile to prepare a shallow wedge type structure in an organic thin film of Irganox 1010 doped with four delta layers of Irganox 3114. This sample has been studied extensively by Shard and co-workers<sup>9</sup> and has been utilized as a standard reference material for a round-robin VAMAS study of molecular depth profiling. The wedge experiments not only reveal a complementary strategy for determining interface widths but also provide direct information about topography and sputtering yield at every point in the depth profile from a single measurement. These data are essential to acquire in order to find optimum parameters for three-dimensional imaging and for making accurate calculations of the ultimate achievable depth resolution.

The experiments were performed using a TOF-SIMS spectrometer<sup>10</sup> equipped with a fullerene ion source delivering a focused ( $\sim 7 \mu$ m diameter) 40 keV C<sub>60</sub><sup>+</sup> ion beam of about 200 pA. A 50 ns primary beam pulse incident at 40° was employed

\* To whom correspondence should be addressed. E-mail: nxw@psu.edu.

<sup>†</sup> Pennsylvania State University.

<sup>‡</sup> University Duisburg-Essen.

(1) Mahoney, C. M.; Roberson, S. V.; Gillen, G. *Anal. Chem.* **2004**, *76*, 3199–3207.

(2) Cheng, J.; Wucher, A.; Winograd, N. *J. Phys. Chem. B* **2006**, *110*, 8329–8336.

(3) Wucher, A.; Cheng, J.; Zheng, L.; Winograd, N. *Anal. Bioanal. Chem.* **2009**, *393*, 1835–1842.

(4) Wucher, A.; Cheng, J.; Zheng, L.; Willingham, D.; Winograd, N. *Appl. Surf. Sci.* **2008**, *255*, 984–986.

(5) Zheng, L.; Wucher, A.; Winograd, N. *Anal. Chem.* **2008**, *80*, 7363–7371.

(6) Hofmann, S. *Surf. Interface Anal.* **1994**, *21*, 673–678.

(7) Gillen, G.; Wight, S.; Chi, P.; Fahey, A.; Verkouteren, J.; Windsor, E.; Fenner, D. B. *AIP Conf. Proc.* **2003**, *683*, 710–714.

(8) Gillen, G.; Fahey, A.; Wagner, M.; Mahoney, C. M. *Appl. Surf. Sci.* **2006**, *252*, 6537–6541.

(9) Shard, A. G.; Green, F. M.; Brewer, P. J.; Seah, M. P.; Gilmore, I. S. *J. Phys. Chem. B* **2008**, *112*, 2596–2605.

(10) Braun, M. R.; Blenkinsopp, P.; Mullock, J. S.; Corlett, C.; Willey, F. K.; Vickerman, C. J.; Winograd, N. *Rapid Commun. Mass Spectrom.* **1998**, *12*, 1246–1252.

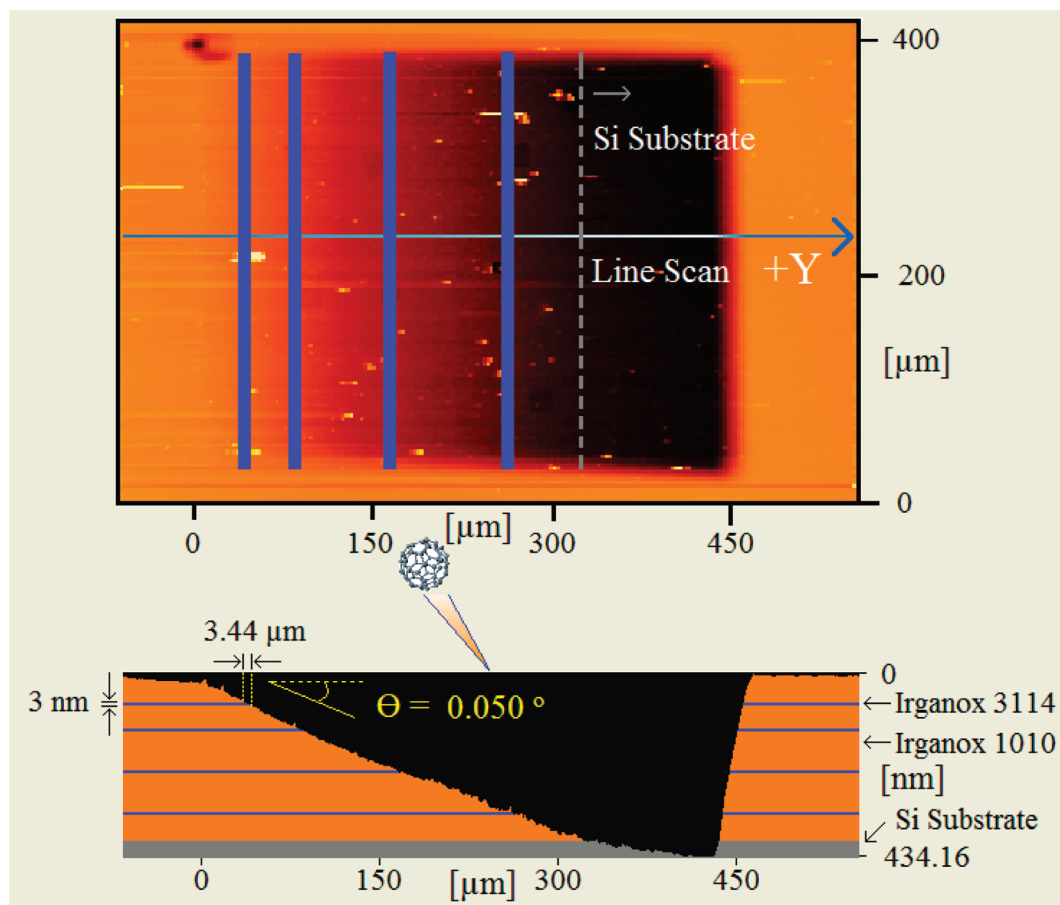


**Figure 1.** AFM image of the wedge crater eroded into a 395 nm Irganox 1010 film on Si doped with four delta layers of Irganox 3114. The upper panel represents a top view with the dark blue vertical lines representing the expected positions of the delta layers. The horizontal light blue line denotes the position of a line scan shown in the bottom panel. In the bottom panel, the position of the delta layers is also shown. With the wedge angle reported as  $0.05^\circ$ , the 3 nm delta layer is expected to appear to be  $3.44 \mu\text{m}$  to the interrogating  $\text{C}_{60}^+$  probe. Note the decrease in the slope of the bevel as the crater reaches the Si substrate, designated in gray. This wedge crater was created by etching for 200 s.

to acquire SIMS spectra. Images were created with a digitally controlled raster over  $256 \times 256$  pixels covering a surface area of  $450 \times 360 \mu\text{m}^2$ . During ion erosion cycles, the beam was operated in a dc mode and rastered across the same field of view as employed for data acquisition. The raster scheme was set up as a sequence of fast frames with a relatively short dwell time of about  $10 \mu\text{s}$  on each pixel. This protocol minimizes material redeposition effects well-known from FIB technology.<sup>5</sup> In order to erode a wedge-shaped crater, the raster area was varied from frame to frame by sequentially skipping more and more lines along the direction of the wedge  $y$ , beginning with the line closest to the ion source. Each time the number of skipped lines reached the total value of 256, the complete raster frame was restored and the sequence repeated. This way, the applied ion fluence varies linearly with ( $y$ ) as

$$f(y) = 2f_0 \frac{y}{L_y} \quad (1)$$

where  $L_y$  is the crater dimension in the  $y$ -direction ( $450 \mu\text{m}$ ) and  $f_0$  is the average applied ion fluence. Since the angle of the beveled structure with respect to the sample surface is always less than  $0.05^\circ$ , the angle of incidence of the primary ion beam remains essentially fixed during the measurement.

More details regarding the creation of the wedge structures are provided in the Supporting Information.

After completion of the crater erosion, the topography of the bombarded surface was investigated using a wide-area AFM (KLA Tencor Nanopics 2100). The system was operated both in contact mode to characterize the erosion crater and noncontact mode to determine the rms surface roughness. Care was taken to correct the obtained images for curvature effects by making sure that line scans taken outside of and parallel to the eroded crater were flat. Measurements were recorded immediately after the wedge was created.

A 395 nm thin film of Irganox 1010 on Si and doped with four delta layers of Irganox 3114 with thicknesses ranging from 3.0 to 3.7 nm served as the model system for these experiments. The sample was manufactured at the National Physical Laboratory (NPL) in the U.K. and was used as received without any further preparation. The four delta layers were created 47, 97, 194, and 293 nm below the surface.

Implementation of a wedge-shaped erosion pattern, combined with the topological precision of AFM, allows the fundamental parameters associated with molecular depth profiling to be acquired with an unprecedented level of detail. To illustrate, the AFM image of the eroded crater for the Irganox model film is shown in Figure 1, and the combined AFM/SIMS information is

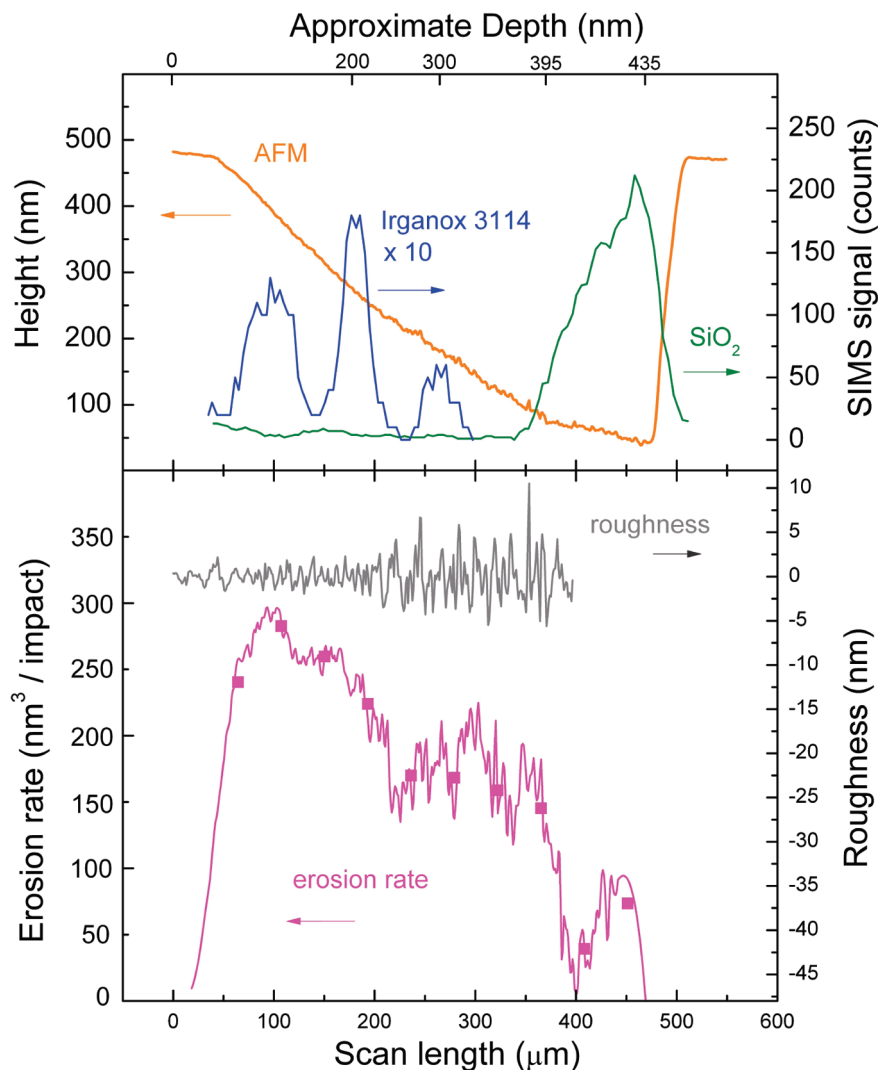


**Figure 2.** The top panel shows a topography scan across the wedge crater along the line indicated in Figure 1 (orange) along with line scans of the SIMS signals representing the Irganox 3114 delta layers ( $m/z$  42, blue) and SiO<sub>2</sub> substrate interface layer ( $m/z$  60, green). The erosion rate is shown in the lower panel in magenta, with smoothed values given by square magenta points. The gray line represents the roughness fluctuations around the average height (see text).

summarized in Figure 2. The data show that it is possible to acquire information about depth resolution using the laterally magnified cross sections during SIMS acquisitions, as well as about erosion rates and topography as a function of primary ion fluence from AFM measurements, all from a single experiment. These parameters are essential to characterize the quality of the depth profile using the previously developed erosion dynamics model.

The AFM pictures depicted in Figure 1 show the top view and a line scan of the beveled crater after erosion is complete. Since the rastering scheme ensures a linear fluence variation according to eq 1, the slope of the crater bottom along this line reflects the erosion rate at the corresponding crater depth. Since this line does not decrease in a linear fashion, it is clear that the erosion rate is decreasing with erosion depth, approaching nearly zero at the Irganox/Si interface. Moreover, the topography data exhibit a short-scale fluctuation which increases with increasing depth.

Combined SIMS data and AFM data are illustrated in the two panels shown in Figure 2. The upper panel shows the uncorrected AFM data for the wedge crater as well as SIMS line scans using the characteristic delta layer SIMS ion at  $m/z$  42 and the SiO<sub>2</sub>

ion at  $m/z$  60. The lower panel consists of smoothed AFM topography data and erosion rate information that has been converted to an approximate depth scale directly associated with the cross section of the Irganox film. The SiO<sub>2</sub> SIMS signal is also included for reference purposes. Any uncertainty in the depth scale calibration arises from the presence of topography.

There are a number of interesting features associated with Figure 2. Although the first two Irganox delta layers at a depth of 47 and 97 nm are not resolved as seen in the upper panel, the third and fourth layers are clearly separated. The full width at half maximum (fwhm) of the third delta layer is found to be ~30 nm, in reasonable agreement to the value of 25 nm reported previously, acquired using 30 keV C<sub>60</sub><sup>+</sup> bombardment.<sup>9</sup> The first two delta layers are easily separated, however, by reducing the beveling angle to effectively increase the lateral magnification. These results are provided as Supporting Information. Although these preliminary data suggest that the beveling process yields data directly comparable to depth profiling using flat-bottomed craters, more experiments will be required to ensure that subtle differences do not exist.

Next, it is possible to calculate the erosion rate from the numerical derivative of the topographical line scan data. Because of the overlaid roughness fluctuations, the resulting magenta curve is quite noisy. Since topography variations generally occur over several nanometers of depth, the fluctuations were smoothed using a 10 point Fourier transform filter (cutoff frequency 0.046). The resulting data are plotted in magenta in the lower panel of Figure 2 and show that the erosion rate drops by roughly a factor of 2 during removal of the Irganox film. This finding is in good agreement with previous data<sup>9</sup> for a similar sample bombarded with 30 keV C<sub>60</sub><sup>3+</sup> ions.

The interface to the underlying substrate is clearly visible by the rise of the substrate related signal in Figure 2. Inspection of the positive secondary ion spectrum in this region reveals a series of strong peaks at  $m/z$  16, 60, 76, 136, and 196, which are interpreted as (SiO<sub>2</sub>)<sub>n</sub>O<sup>+</sup> secondary cluster ions originating from the native oxide layer between the molecular film and the silicon substrate. At the interface, the erosion rate is found to abruptly drop to nearly zero, reflecting the fact that the sputter yield of SiO<sub>2</sub> is significantly lower than that of the organic film.

The data presented in Figure 2 can be used to settle a long-standing question<sup>11</sup> regarding the erosion rate variation across various interfaces. It is seen that an initial, rather abrupt stoppage of the erosion occurs at the point where the SiO<sub>2</sub><sup>+</sup> ion signal has reached about 25% of its maximum value. Interestingly, the erosion rate appears to pick up again within the interface oxide layer, until it stops when the Si substrate is reached. The average erosion rate throughout the removal of the interface oxide layer is about 20% of that of the Irganox film immediately before reaching the interface. A linear interpolation based on the variation of the substrate signal, as is often used to correct for interface variations,<sup>12–15</sup> would result in a value of approximately 50% and therefore lead to a slight overestimation of the actual interface width.

In order to evaluate the development of surface roughness, the topography scan is first smoothed by a 36-point Savitzky–Golay algorithm. The resulting data represent the average height of the crater bottom at each point along the scan. Subtracting this curve from the original line scan data then yields the height fluctuations

which represent the surface roughness. These data are shown as the gray trace in the lower panel of Figure 2 and reveal that the surface roughness increases with increasing crater depth. Starting from an initial surface value below 1 nm, the roughness increases only slightly up to an eroded depth of about 200 nm. At this point, which interestingly coincides with the removal of the third Irganox 3114 delta layer, the roughness suddenly builds up. At the same time, relatively large fluctuations of the topography are observed, which appear to be correlated with corresponding fluctuations of the erosion rate as well. After erosion to a depth of about 395 nm, a roughness value of about 4 nm is reached. This type of information would be extremely tedious to obtain from conventional depth profiling experiments since AFM measurements would be required at many depths.

In summary, we show that the wedge crater provides a simple means to obtain valuable information about depth resolution, topography, and the depth dependence of the erosion rate in molecular sputter depth profiling. This information is required to allow an accurate calibration of the depth scale in such experiments. There are important implications associated with this preliminary study. For biomaterials such as single cells and tissue, the beveling approach may provide a better means for directly observing the bilayer associated with cell membranes. Moreover, dramatic changes in topography and erosion rate are expected for such complex systems, complicating the construction of three-dimensional mass spectral information. A direct point by point determination of the factors that influence the depth scale would provide a direct means of correcting for these important effects.

## ACKNOWLEDGMENT

Financial support from the National Institute of Health under Grant No. 2R01 EB002016-16 and LipidMaps consortium GM 069338-07, the National Science Foundation under Grant No. CHE-0908226, and the Department of Energy Grant No. DE-FG02-06ER15803 is acknowledged. The authors are grateful to Alex Shard for providing the delta-layer sample.

## SUPPORTING INFORMATION AVAILABLE

Additional information as noted in text. This material is available free of charge via the Internet at <http://pubs.acs.org>.

Received for review October 13, 2009. Accepted November 23, 2009.

AC902313Q

(11) Jiang, X.; Alkemade, A. *J. Vac. Sci. Technol., B* **1998**, *16*, 1971–1982.

(12) Cheng, J.; Winograd, N. *Anal. Chem.* **2005**, *77*, 3651–3659.

(13) Wagner, S. M. *Anal. Chem.* **2004**, *76*, 1264–1272.

(14) Wucher, A.; Cheng, J.; Winograd, N. *Appl. Surf. Sci.* **2008**, *255*, 959–961.

(15) Wucher, A.; Winograd, N. *Anal. Bioanal. Chem.* **2009**, in press.